

Study on Poly(3,4-ethylene dioxythiophene)-Poly(styrenesulfonate) as a plastic counter electrode in dye sensitized solar cells

A. KANCIURZEWSKA^a, E. DOBRUCHOWSKA^{a,b}, A. BARANZAHİ^a, E. CARLEGRİM^a, M. FAHLMAN^a, M. A. GÎRȚU^{c*}

^aDepartment of Science and Technology, Linköping University, S-60174 Norrköping, Sweden

^bDepartment of Molecular Physics, Technical University of Lodz, 90-924 Lodz, Poland

^cDepartment of Physics, Ovidius University of Constanța, 900527 Constanța, Romania

Dye sensitized solar cells with PEDOT-PSS coated directly on flexible polyester substrate as counter electrode have been fabricated. The behavior of such plastic counter electrode in the presence of I^-/I_3^- redox electrolyte has been investigated with X-ray photoelectron spectroscopy. We have found that some of iodine species are "trapped" within the PEDOT-PSS layer. The presence of I_3^- , I_2 and PEDOT charge transfer complexes with iodine species may block the surface of the electrode. Furthermore, the PEDOT may be further oxidized (p-doped) during cell operation, which in turn may cause overoxidation and loss of conductivity in the PEDOT-PSS film. Additionally, the interactions between PEDOT and iodine species may be enlarged because of the partial loss of PSS protective counter ion. That has resulted in decrease of PEDOT-PSS catalytic activity for reduction of I_3^- to I^- in the redox electrolyte and has caused worse cell performance than in case of DSSC with Pt counter electrode.

(Received November 2, 2006; accepted February 28, 2007)

Keywords: Dye-sensitized solar cells, plastic counter electrode, PEDOT-PSS, photoelectron spectroscopy.

1. Introduction

Dye-sensitized solar cells (DSSCs) have attracted worldwide attention since the breakthrough report of O'Regan and Grätzel [1]. The concept is still considered as a promising future technology, which is based on the use of inexpensive components and relatively simple production technology. A typical DSSC consist of nanocrystalline TiO_2 electrode covered with a mono-layer of sensitizing dye, a redox electrolyte (e.g. I^-/I_3^-) and a counter electrode such as platinized conductive glass. Working principles of the device have been described in detail in many articles and reviews [2, 3]. In general, a sensitizer anchored to the surface of TiO_2 absorbs the light, and charge separation occurs at the interface by photo-induced electron injection from the dye into the conduction band of TiO_2 . Carriers then are transported to the charge collector. The original state of the sensitizer is restored by electron donation from redox system. The iodide ion, donating an electrode to the sensitizing dye, is regenerated in turn by reduction of triiodide ion at the counter electrode.

Platinum is known to possess high catalytic activity for reduction of I_3^- to I^- in the redox electrolyte, which is necessary, as described above, for proper cell's performance, high conductivity and high stability. On the other hand, Pt is one of the expensive component materials in DSSC [4]. Therefore, the use of non-insulating plastic materials, which belong to the class of so-called conjugated polymers, instead of Pt is expected to reduce

production costs, particularly in case of large-scale manufacturing.

Among the conjugated polymers, poly(3,4-ethylenedioxythiophene) (PEDOT) is one of the most attractive materials for device construction, due to its excellent conducting and electro-optical properties. Prepared *via* standard oxidative chemical or electrochemical polymerization, PEDOT is an insoluble polymer with very high conductivity (ca. 550 S cm^{-1}), high transparency in visible range and remarkable stability at room temperature [5, 6]. Its solubility problem can be solved by using a water-dispersible polyelectrolyte, poly(styrenesulfonic acid) (PSSH), as the charge-balancing dopant during polymerization, yielding PEDOT-PSS (see Fig.1 (a)). This material, displaying good film-forming properties and good conductivity (ca. 10 S cm^{-1}), has been already used in several applications including polymer light emitting diodes [7], field effect transistors [8,9], solid electrolyte capacitors [10], antistatic coatings in photographic films (AGFA), etc. Recently, several attempts have been undertaken to apply PEDOT in dye-sensitized solar cells. Saito *et al.* [11,12] fabricated solar cells using chemically polymerized poly(3,4-ethylenedioxythiophene) on a conductive glass as a counter electrode, which showed comparable efficiency to cells based on platinum sputtered counter electrode. Johansson *et al.* investigated TiO_2 /dye/PEDOT-PSS systems where TiO_2 acting as an electron conducting material and PEDOT-PSS acting as a hole transport material [13]. In the present work, we checked the performance of DSSCs with commercially available

PEDOT-PSS coated on flexible polyester substrate, since the next generation of solar cells will probably be based on thin organic film technology due to its potential for lower production costs. Moreover, flexible electrodes present some other advantages, relative to electrodes on glass

substrate, e.g. lower weight, impact resistance and less form and shape limitation. However, our main attention was focused on studies of behavior of such plastic counter electrode in the presence of I^-/I_3^- redox electrolyte, since iodide/triiodide is the common choice

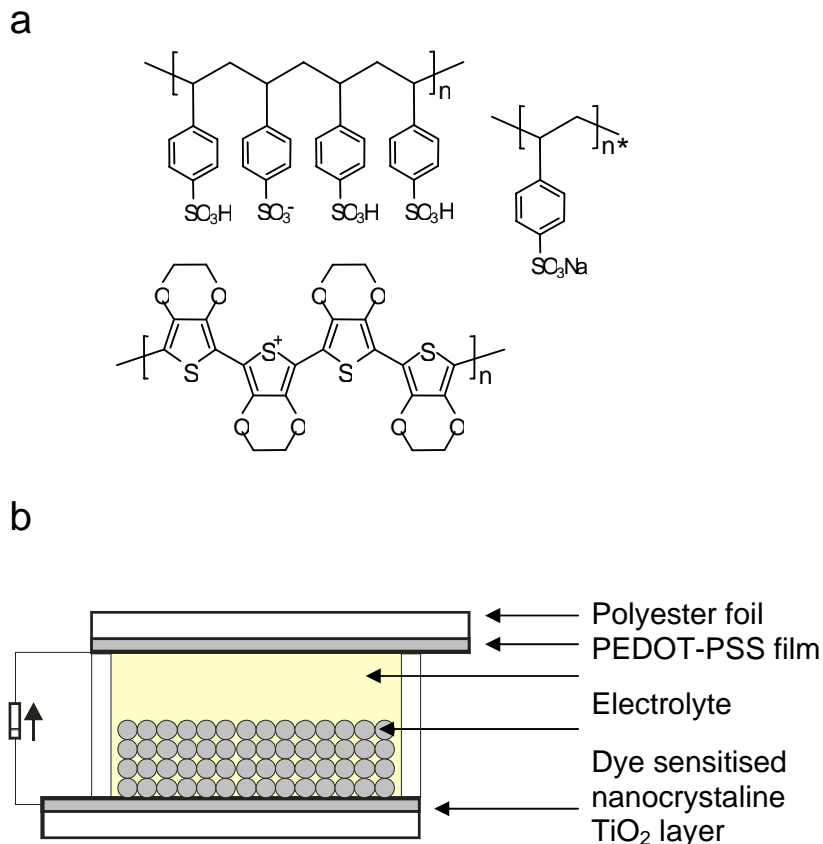


Fig. 1. The chemical formula of PEDOT-PSS, displaying the different species PEDOT, PSS^{-H⁺}, PSS^{-Na⁺} (a) and the basic structure of the device used (b).

of redox couple for obtaining high efficiencies in liquid electrolytes. In order to probe chemical and electronic properties of PEDOT-PSS foil, X-ray photoelectron spectroscopy was used as a powerful tool to study the atomic composition of the surface.

2. Experimental details

2.1. Sample preparation

Fig. 1 (b) shows the device configuration of investigated dye-sensitized solar cells. For preparation of nanocrystalline TiO₂ photoelectrode, a small amount of TiO₂ suspension (Ti nanoxide-T: colloidal anatase, particle size of ~13 nm, Solaronix, Switzerland) was applied onto a conductive glass by doctor blading using adhesive tape (thickness ~41 μm) as a frame and spacer. The conductive glass substrate was the Tec 8 supplied by Hartford Glass and consisted of a soda lime glass sheet with the conductive layer of F-doped SnO₂ (sheet resistance: 8

Ω/square). After evaporation of solvent from the deposited suspension, the substrate with the obtained film was sintered for 30 min at 450°C in the oven. The thickness of the TiO₂ was around 5 μm. Subsequently, the TiO₂ electrode was dye sensitized by immersion for 24 h in 0.5 mM tris(isothiocyanato)-ruthenium(II)-2,2':6',2''-terpyridine-4,4',4''-tricarboxylic acid, tris-tertrabutyl-ammonium salt (Ruthenium 620-1H3TBA, Solaronix) solution in absolute ethanol, rinsed with ethanol and dried. The counter electrode consisted of 0.2 μm thick PEDOT-PSS film (Orgacon™) coated on flexible polyester foil supplied by AGFA-Gevaert, Mortsel, Belgium. The PEDOT-PSS/polyester foil was used as delivered for all experiments carried out in the frame of this work. The two described above electrodes were clipped together to make a sandwich type cell. The electrolyte was injected into the space between the electrodes and filled the nanocrystalline TiO₂ layer through a capillary action. The electrolyte solution was composed of 0.5 M of KI and 0.05 M of iodine in tetraethylene glycol dimethyl ether (Solaronix).

The cell with the counter electrode consisted of a thermally platinized conductive glass (5 mM H_2PtCl_6 in dry isopropanol, heated at 380°C on a conductive glass substrate for 10 min) was used as a reference sample.

2.2. Measurements

The photo-electrochemical properties of DSSCs were studied by measuring the photocurrent-voltage (I - V) characteristics under white-light (100 mW/cm^2) irradiation using halogen lamp (Xenophot, Osram). The I - V curves were monitored with a digital source meter (Keithley Model 2400).

X-ray photoelectron spectroscopy (XPS) was applied in order to study the atomic composition of surface and bulk of PEDOT-PSS films used as counter electrodes in DSSCs. The measurements were performed using a Scienta® ESCA200 spectrometer, with a base pressure of $1 \cdot 10^{-10}$ mbar (UHV), using monochromatized $\text{Al}(\text{K}\alpha)$ X-rays, at $h\nu=1486.6 \text{ eV}$. The energy pass was set at 500 eV for all experiments. The experimental conditions were such that the Full Width at Half Maximum (FWHM) of the gold $\text{Au}(4f_{7/2})$ line was 0.65 eV . High-resolution scans with a good signal ratio were obtained in the C(1s), S(2p), O(1s), F(1s), K(2p), Na(1s) and I(3d_{5/2}) regions of the spectrum. The quantitative analysis was based on the determination of C(1s), S(2p), O(1s), F(1s), K(2p), Na(1s) and I(3d_{5/2}) peak areas. All the spectra were recorded under identical condition. Samples were analyzed at two angles (0° and 60°) with respect to the film surface in order to more bulk or surface sensitive, respectively. The devolution of the XPS peaks into different components and quantitative interpretation were made after subtraction of the background using the Shirley method [14]. The developed curve-fitting programs permitted the variation of the parameters such as Gaussian/Lorentzian ratio, the full width at half maximum (FWHM), the position and intensity of the contribution. These parameters were optimized by a curve-fitting program in order to obtain the best fit of the experimental curves.

3. Results and discussion

Fig. 2 shows photocurrent-voltage curves for cells with PEDOT-PSS/polyester and Pt counter electrode under irradiation of 100 mW/cm^2 . The parameters typical of the cells are listed in Table 1. The overall conversion efficiency (η) has been calculated using the following equation:

$$\eta = ff \frac{V_{\text{OC}}(\text{V}) \times I_{\text{SC}}(\text{mA/cm}^2)}{P_{\text{inc}}(\text{mW/cm}^2)}, \quad (1)$$

where V_{OC} , I_{SC} , ff , and P_{inc} are the open circuit potential, short circuit current, fill factor, and incident light power, respectively. The value of the fill factor of the device has been determined by calculating the area of the maximum

power rectangular area under I - V curve. Therefore, the fill factor is given by:

$$ff = \frac{V_{\text{max}} \times I_{\text{max}}}{V_{\text{OC}} \times I_{\text{SC}}}, \quad (2)$$

where V_{max} and I_{max} are the voltage and current, respectively, at the point of maximum power output.

One can notice, that DSSCs with PEDOT-PSS/polyester counter electrode exhibit much lower values of I_{SC} , ff , and as a result lower efficiency in comparison to those where Pt electrode was applied. On the other hand, Saito *et al.* [11] observed

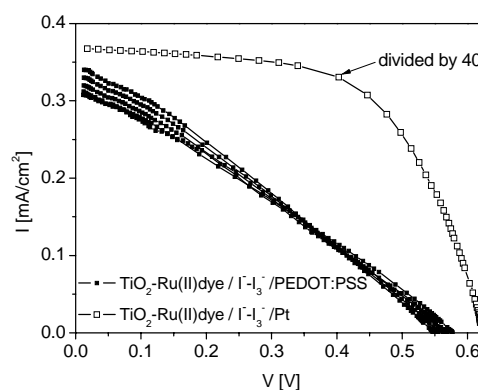


Fig. 2. Photocurrent-voltage curves for cells with PEDOT-PSS and Pt (the average curve for five DSSCs) as counter electrodes under 100 mW/cm^2 irradiation. For better look the current values obtained for DSSC with Pt counter electrode were divided by factor 40.

Table 1. Characteristic parameters of the investigated DSSCs.

Counter electrode	V_{OC} [V]	I_{SC} [mA/cm^2]	ff	η [%]
PEDOT-PSS/polyester ^(a)	0.56 ± 0.01	0.32 ± 0.02	0.29 ± 0.00	$5.2 \times 10^{-2} \pm 0.4 \times 10^{-2}$
PEDOT-PSS/conductive glass ^(b)	0.68	11.00	0.28	2.10
Pt/conductive glass ^(a)	0.62 ± 0.01	14.69 ± 0.38	0.60 ± 0.05	5.50 ± 0.79

- (a) The table shows average values for five DSSCs (see I - V curves in Fig.2).
 (b) The literature data [9]. The cells were measured under conditions similar to these used in the current work.

comparable V_{OC} , I_{SC} and only lower ff for cells with PEDOT-PSS deposited on conductive glass. However, in case of our measurements, PEDOT-PSS was supposed to act as an independent (plastic) electrode, since it was applied directly on the polyester substrate without any additional layer of inorganic semiconductor like ITO or

F:SnO₂. Thus, worse cell performance can result from lower ability of PEDOT-PSS to I₃⁻ reduction or be due to insufficient transport of charge carriers to the external circuit (which could lead to decrease of *ff*). In order to check whether any chemical or physical changes (like charge transfer complexes creation between oppositely charged species) occur in PEDOT-PSS film in contact with electrolyte during cell operation, XPS studies were carried out

Fig. 3 shows XPS wide scans that give bulk elemental composition of PEDOT-PSS/polyester foil recorded for both; pristine samples (see Fig. 3 (a)) and samples used as a counter electrode in DSSC (see Fig. 3 (b)). Results of the quantitative analysis are reported in Table II. One can see that pristine PEDOT-PSS films contain features corresponding to carbon,

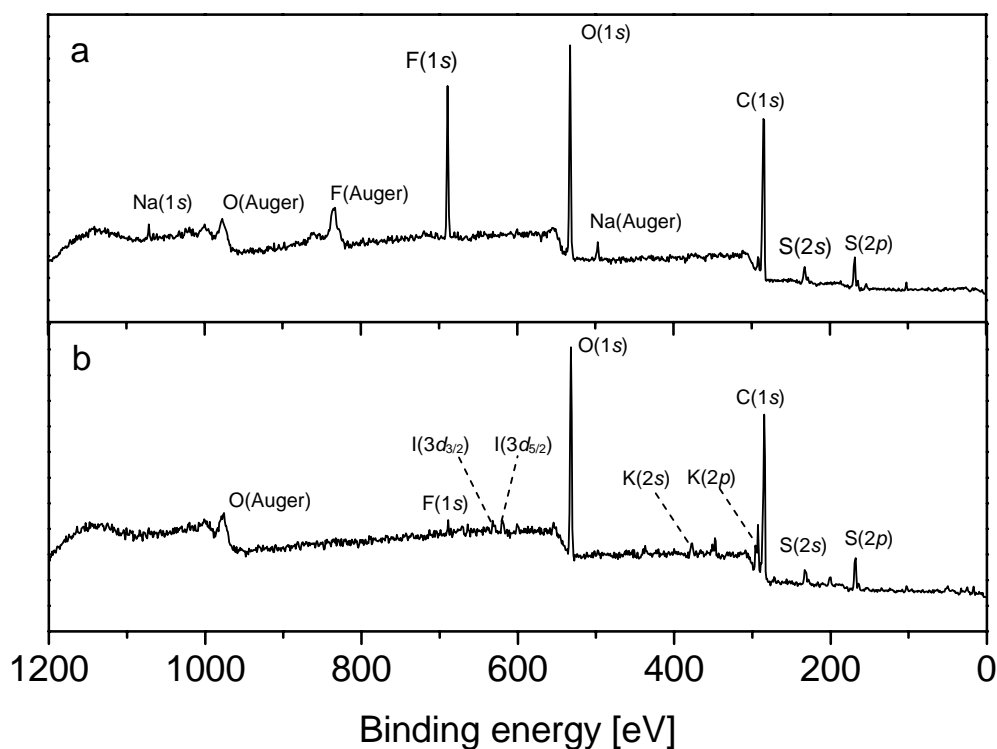


Fig. 3. XPS wide scan giving the bulk elemental composition of PEDOT-PSS film on polyester foil recorded for pristine sample (a) and used as a counter electrode (b).

Table 2. XPS quantitative analyses.

Atomic %	Pristine PEDOT-PSS	PEDOT-PSS used as a counter electrode
C	58	57
O	24	29
S	7	9
F	10	0.5
Na	1	0
K	0	4
I	0	0.5

sulfur, and oxygen (elements present in PEDOT-PSS molecules) as well as sodium and fluorine. The latter two elements are expected as fluorine-containing species are present in the commercial Orgacon™ foil and sodium contamination typically occurs due to exchange of the proton for a sodium at some of the SO₃H⁺ units of the PSSH.

After operation of a device, changes occur to the stoichiometry of the films. The concentration of the fluorine anion is much lower after use in solar cell. We propose that the fluorine-containing molecules migrate through PEDOT-PSS film and are removed by liquid electrolyte. Another difference observed in the spectrum for the counter electrode, is complete lack of sodium cations (Na(1s) core level is located at ~1072 eV). On the other hand, a potassium line appears at ~294 eV (K⁺ is

present in redox electrolyte solution). These observations suggest that during cell performance the sodium cations are liberated and further removed or simply exchanged with potassium, creating PSS^-K^+ instead of PSS^-Na^+ . Moreover, as one can see from the data given in Table II, the relative concentration of C, O and S atoms has changed slightly after treatment with electrolyte. Additionally, after contact with electrolyte, the material shows the presence of not only the elements constituting the material but also iodine species.

Fig. 4 presents the $\text{S}(2p)$ spectrum of pristine PEDOT-PSS (a) and used in solar cell (b). As it is known, both PEDOT and PSS contain one sulfur atom per repeated unit. In PEDOT, the sulfur atom is included to the thiophene ring, whereas in case of PSS, it is a part of the sulfonate moiety. Because of these different chemical environments, the $\text{S}(2p)$ electrons of PEDOT and PSS have different binding energies and therefore the composition of PEDOT-PSS can be analyzed by XPS. The $\text{S}(2p)$ core level feature of PEDOT-PSS has been described in detail elsewhere [15]. The spin-split doublet peak from the sulfur originating from the PSS chains has its maximum at roughly ~ 168.5 eV, whereas the spin-split doublet originating from the PEDOT chains has its maximum located ~ 164.0 eV. The PEDOT sulfur doublet is asymmetric and tails of towards higher binding energy due to the different charge environments induced by the p-doping of the sulfur atoms in the thiophene rings of the PEDOT chains [15]. The intensity ratio between the signal from PSS and PEDOT gives directly the $R_{\text{S/T}}$ ratio. The $R_{\text{S/T}}$ value found for pristine PEDOT-PSS equals 0.34, whereas for sample used as a counter electrode $R_{\text{S/T}}$ is lower and amounts 0.26.

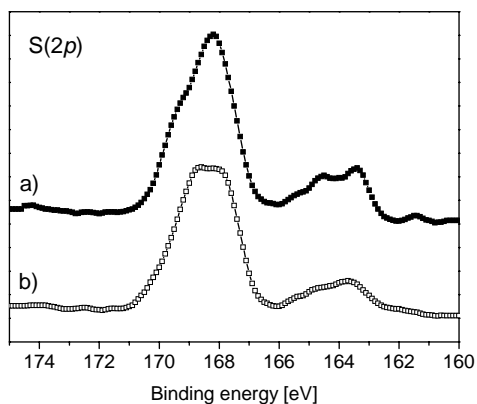


Fig. 4. $\text{S}(2p)$ core level XPS spectra of PEDOT-PSS film on polyester foil recorded for pristine sample (a) and used as a counter electrode (b).

A change in this ratio is an indication that the PEDOT-PSS morphology is modified after the use as a counter electrode in solar cell. The decrease of the total PSS-to-PEDOT ratio implies that a part of the PSS is actually washed away in contact with the electrolyte. For the $\text{S}(2p)$ core level spectra shown in Fig. 4(b), there is a

broadening towards higher binding energy in the PSS-derived features. This could indicate that SO_3^-Na^+ and SO_3^-H^+ groups are transformed into SO_3^-K^+ through ion exchange upon exposure to the electrolyte. This is consistent with the stoichiometry data displayed in Table 2. The asymmetry of the tail of the spin split doublet associated to the PEDOT sulfur is enhanced after operating the device, suggesting that the doping level of the PEDOT has been changed.

The $\text{O}(1s)$ core level spectrum for pristine PEDOT-PSS (a) and PEDOT-PSS used as a counter electrode (b) is shown in Fig. 5. The peak at higher binding energy (~ 533 eV) corresponds to the oxygen from the PEDOT chain and at the high binding energy contribution of PSSH. The peak at lower binding energy ~ 531 eV corresponds to the low binding energy contribution of PSSH as well as to contribution of PSSNa [15]. When comparing the PEDOT and PSS part of the PEDOT-PSS $\text{O}(1s)$ feature for pristine sample and used as a counter electrode small differences can be discerned. First of all, the peak at higher binding energy corresponding to the hydroxyl-oxygen atoms in PSSH (~ 533 eV) is broadened. Moreover, peak at ~ 531 eV is slightly shifted towards lower binding energy. This is consistent with an exchange of H^+ and Na^+ ions for K^+ , as the resulting different chemical environment for the SO_3^- oxygen atoms will produce chemical shifts in the $\text{O}(1s)$ core level features.

In the $\text{C}(1s)$ core level spectra shown in Fig. 6, there are two main features: a strong peak at lower binding energy which corresponds to carbon atoms bonded to sulfur and aromatic carbon atoms, and a broad shoulder at higher binding energy. The broad shoulder extending to ~ 3 eV above the main peak corresponds to carbon atoms bonded to oxygen as well as a $\pi-\pi^*$ shake-up process of the PEDOT chains [16]. There are no significant changes in the $\text{C}(1s)$ spectra after operation of the devices though a slight shift towards higher binding energy for the main peak is observed (see Fig. 6b).

The stoichiometry results showed that iodine appears in the PEDOT-PSS films after the solar cells have been operated. The presence of iodine species is indicated by the $\text{I}(3d_{5/2})$ peak appearing at ~ 619 eV. We performed XPS measurements in both surface and bulk sensitive mode of the PEDOT-PSS films in order to check for iodine species migration into the polymer counter electrode. It is possible to be more surface sensitive by tilting the sample (takeoff-angle $\text{TOA}=60^\circ$) during the XPS measurements since then only the photoelectrons coming from a depth about 30 \AA (95% of the signal) in the organic film are collected, while for $\text{TOA}=0^\circ$ (bulk mode) XPS probes down to $\sim 70 \text{ \AA}$ (95% of the signal). The high-resolution $\text{I}(3d_{5/2})$ XPS spectra can be deconvoluted into three peaks as shown in Fig. 7 for bulk (a) and surface (b). That suggests the presence of multiple charge states of iodine in the sample. Results from peak deconvolution of $\text{I}(3d_{5/2})$ spectrum are displayed in Fig. 7 and the binding energies of the individual peaks correspond well to literature data [17-22]. We assign the

peak of the binding energy at 618.4 eV to I_3^- , and the peak of the binding energy at 620.4 eV to I_2^- . The relative concentration of I_3^- to I_2^- is slightly larger in the bulk than at the surface.

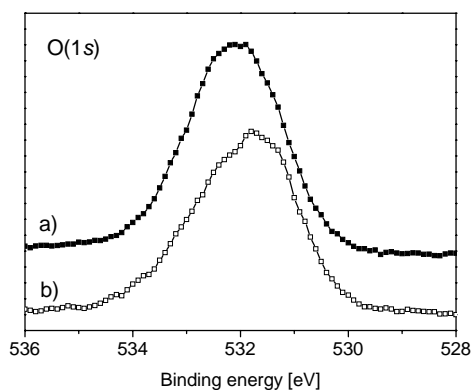


Fig. 5. $O(1s)$ core level XPS spectra of PEDOT-PSS film on polyester foil recorded for pristine sample (a) and used as a counter electrode (b).

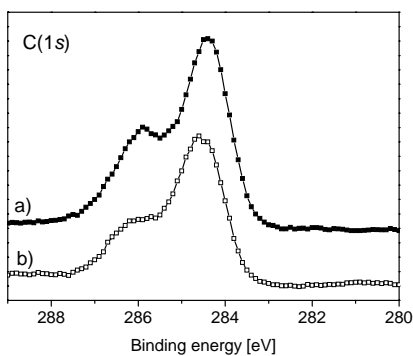


Fig. 6. $C(1s)$ core level XPS spectra of PEDOT-PSS film on polyester foil recorded for pristine sample (a) and used as a counter electrode (b).

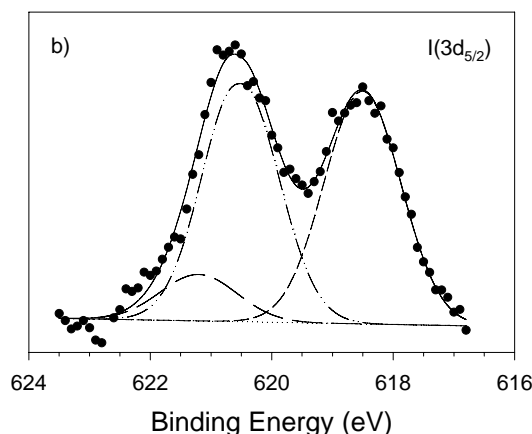
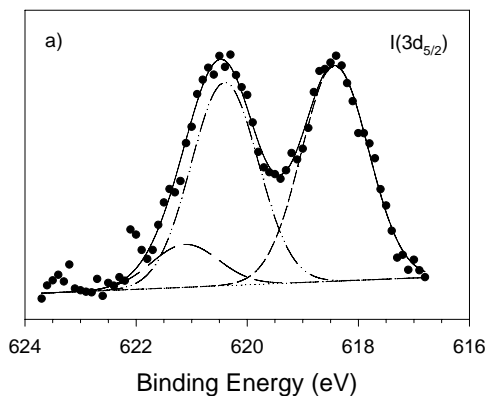


Fig. 7. $I(3d_{5/2})$ core level XPS spectra of PEDOT-PSS film on polyester foil used as a counter electrode, recorded for bulk (a) and surface (b). The dots represent the data points, the solid lines correspond to peak fits obtained by deconvolution procedure using the Gaussian analysis.

The binding energy of I_3^- is nearly identical to I_3^- that has p-doped model molecules of PEDOT [19]. This suggests that PEDOT possess some ability to form charge-transfer complexes with iodine, which also has been proposed by Biallozor *et al* [23] on the base of cyclic voltammetry measurements. Hence, we conclude that after operating the solar cells, there is I_3^- (and I_2^-) at the interface and in the bulk of the PEDOT-PSS foil.

The origin of the peak of higher binding energy at 621.1 eV is unclear. This $I(3d_{5/2})$ binding energy could indicate an iodine environment associated with electron withdrawing atoms, as proposed by Tang *et al.* [17] and Mengoli *et al.* [24] in their studies on formation of polyaniline-iodine charge transfer complexes. Formation of PANI-iodine charge transfer complexes was investigated by cyclic voltammetry of KI/polyaniline-film Pt electrodes and XPS analysis for PANI samples doped with iodine. Tang, *et al.*, have suggested that the iodine species interact with the PANI chains and form donor-acceptor complex between the iodine species and the N atoms, resulting in high binding energy features (621.3 eV and 622.3 eV) of the $I(3d_{5/2})$ core level spectrum [17]. However, it is unlikely that this is the case for the PEDOT-PSS system as there is no likely electron-withdrawing group available for such reaction. We instead propose that the high binding energy feature at 621.1 eV originates from a shake-up process involving the PEDOT polymer. For iodine species complexed to the PEDOT chains, the emission of an $I(3d_{5/2})$ core level electron may lead to a final state where a $\pi-\pi^*$ transition (shake-up) of the PEDOT electronic structure has taken place. The appearance of a $C(1s)$ $\pi-\pi^*$ shake up from a conjugated polymer on the iodine 3d core level spectrum has been demonstrated for iodine-doped polyacetylene [23]. The shift of the high energy peak at 621.1 eV compared to the I_3^- feature is 2.7 eV, in good agreement with the shake-up energy of $C(1s)$ spectrum in Fig. 6 and the shake-up

energy of a three-ring PEDOT oligomer (2.9 eV) [16]. There is no such shake-up peak associated with the I_2 peak, which is reasonable as the I_2 molecules are unlikely to strongly interact with the PEDOT polymers.

The presence of I_3^- coordinated to PEDOT, could be the result from electrochemical process where the PEDOT is increasingly p-doped during driving of the cell. The I_3^- would then act as counter ions in the process. PEDOT-PSS films can suffer reduction in conductivity due to overoxidation, and such process can occur even upon exposure to an electrolyte without the presence of a field. It is thus likely that the PEDOT-PSS film is degraded during driving of the solar cell and cell performance will be (progressively) worse than if a Pt electrode was used instead. The presence of I_3^- , as well as I_2 , at the surface of the investigated films may block the external surface of the electrode. That would result in the decrease of PEDOT-PSS catalytic activity for reduction of I_3^- to I^- in the redox electrolyte and causes worse cell performance than in case of DSSC with Pt counter electrode.

4. Conclusions

Dye sensitized solar cells, with PEDOT-PSS coated by a flexible polyester substrate serving as the counter electrode, were fabricated. One can expect that PEDOT-PSS electrode would be efficient enough to guarantee good cell performance when ionic liquid is used for the electrolyte, because of its porous structure and thus an increased active surface. However, we have found that some of iodine species diffusing from the bulk of solution to the electrode surface and further through the polymer film are "trapped" within the PEDOT-PSS layer. The presence of I_3^- , I_2 and PEDOT charge transfer complexes with iodine species in the investigated material may block the surface of the electrode. Furthermore, the PEDOT may be further oxidized (p-doped) during cell operation, which in turn may cause overoxidation and loss of conductivity in the PEDOT-PSS film. Additionally, the interactions between PEDOT and iodine species may be enlarged because of the partial loss of PSS protective counter ion. That results in the decrease of PEDOT-PSS catalytic activity for reduction of I_3^- to I^- in the redox electrolyte and causes worse cell performance than in case of DSSC with Pt counter electrode. For better cell operation, the change of redox mediator, safe for PEDOT-PSS, should be considered.

Acknowledgements

Research in Norrköping was supported by the Swedish Research Council (VR), the Swedish Foundation for Strategic Research funded Center for Organic Electronics, COE@COIN, and Center for Advanced Molecular Materials, CAMM; the Carl Tryggers Foundation, DuPont Displays and RTN-LAMINATE (EU project number 00135). Research in Romania was supported by the Romanian Ministry of Education and Research through the CNCSIS grant A678/2006 and the ANCS grant CEEX-M3-C3-12350.

References

- [1] B. O'Regan, M. Grätzel, *Nature* **353**, 737 (1991).
- [2] D. Cahen, M. Grätzel, J. F. Guillemoles, G. Hodes, in: G. Hodes (Ed.), *Electrochemistry of Nanomaterials*, Wiley-VCH, 2001.
- [3] M. Grätzel, *J. Photochem. Photobiol. A: Chem.* **164**, 3 (2004).
- [4] G. Smestad, C. Bignozzi, R. Argazzi, *Sol. Energy Mater. Sol. Cells* **32**, 259 (1994).
- [5] L. B. Groenendaal, F. Jonas, H. Freitag, H. Pielartzik, J. R. Reynolds, *Adv. Mater.* **12**, 481 (2000).
- [6] L. B. Groenendaal, G. Zotti, P.-H. Aubert, S. M. Waybright, J. R. Reynolds, *Adv. Mater.* **15**, 855 (2003).
- [7] J. S. Kim, M. Granstrom, R. H. Friend, N. Johansson, W. R. Salaneck, R. Daik, W. J. Feast, F. Cacialli, *J. Appl. Phys.* **84**, 6859 (1998).
- [8] H. Sirringhaus, T. Kawase, R. H. Friend, T. Shimoda, M. Inbasekaran, W. Wu, E. P. Wo, *Science* **290**, 2123 (2000).
- [9] G. H. Gelinck, T. C. T. Geunus, D. M. D. Leeuw, *Appl. Phys. Lett.* **77**, 1487 (2000).
- [10] S. Ghosh, O. Inganäs, *Adv. Mat.* **11**, 1214 (1999).
- [11] Y. Saito, W. Kubo, T. Kitamura, Y. Wada, S. Yanagida, *Chem. Lett.* **31**, 1060 (2002).
- [12] Y. Saito, W. Kubo, T. Kitamura, Y. Wada, S. Yanagida, *J. Photochem. Photobiol. A: Chem.* **164**, 153 (2004).
- [13] E. M. J. Johansson, A. Sandell, H. Siegbahn, H. Rensmo, B. Mahrov, G. Boschloo, E. Figgemeier, A. Hagfeldt, S. K. M. Jönsson, M. Fahlman, *Synthetic Metals* (in press).
- [14] D. A. Shirley, *Phys. Rev.* **55**, 4709 (1972).

- [15] G. Greczynski, T. Kugler, and W. R. Salaneck, *Thin Solid Films* **354**, 129 (1999).
- [16] S. K. M. Jönsson, M. P. de Jong, L. Groenendaal, W. R. Salaneck, M. Fahlman, *J. Phys. Chem. B*, **107**, 10793 (2003).
- [17] H. Tang, A. Kitani, M. Shiotani, *J. Appl. Electrochem.* **26**, 36 (1996).
- [18] G. E. Muilenberg (ed.), *Handbook of X-ray Photoelectron Spectroscopy*, Perkin-Elmer, Minneapolis, KS (1979).
- [19] C. Wochnowski, S. Metev, *Appl. Surface Scie.* **186**, 34 (2002).
- [20] J. C. Bernede, H. Taoudi, A. Bonnet, P. Molinie, M. Morsli, M. A. de Valle, F. Diaz, *J. Appl. Polym. Scie.* **71**, 115 (1999).
- [21] M. P. de Jong, A. W. Denier van der Gon, X. Crispin, W. Osikowicz, W. R. Salaneck, L. Groenendaal, *J. Chem. Phys.* **118**, 6495 (2003).
- [22] W. R. Salaneck, H. R. Thomas, R. W. Bigelow, C. B. Duke, E. W. Plummer, A. J. Heeger, A. G. MacDiarmid, *J. Chem. Phys.* **72**, 3674 (1980).
- [23] S. Biallozor, A. Kupniewska, *Electrochem. Commun.* **2**, 480 (2000).
- [24] G. Mengoli, M. M. Musiani, D. Pletcher, S. Valcher, *J. Appl. Electrochem.* **17**, 525 (1987).

*Corresponding author: girtu@univ-ovidius.ro